applied sciences

MDPI

*Article*

# A Simple and Low-Cost Technique for 5G Conservative Human Exposure Assessment

**Fulvio Schettino [1,2,3,*], Gaetano Chirico [1,2,3], Ciro D'Elia [1,3], Mario Lucido [1,2,3], Daniele Pinchera [1,2,3] and Marco Donald Migliore [1,2,3]**

1 DIEI (Dipartimento di Ingegeria Elettrica e dell'Informazione "Maurizio Scarano"), University of Cassino and Southern Lazio, 03043 Cassino, Italy; gaetano.chirico@studentmail.unicas.it (G.C.); lucido@unicas.it (M.L.); pinchera@unicas.it (D.P.); mdmiglio@unicas.it (M.D.M.)
2 ICEmB (Inter-University Research Center on the Interactions between Electromagnetic Fields and Biosystems), University of Cassino and Southern Lazio, Via G. Di Biasio 43, 03043 Cassino, Italy
3 CNIT (National Inter-University Consortium for Telecommunications), University of Cassino and Southern Lazio, Via G. Di Biasio 43, 03043 Cassino, Italy
* Correspondence: schettino@unicas.it; Tel.: +39-0776-299-4310

**Abstract:** The purpose of this paper is to introduce a simple, low-cost methodology for estimating a conservative value of the maximum field level that can be radiated by a 5G base station useful for human exposure assessment. The method is based on a Maximum Power Extrapolation (MPE) approach and requires the measurement of a reference quantity associated with the SS-PBCH, such as Primary Synchronization Signal (PSS), Secondary Synchronization Signal (SSS), Physical Broadcast CHannel (PBCH), or PBCH Demodulation Reference Signal (PBCH-DMRS). This step requires a simple spectrum analyzer and allows one to obtain the Resource Element (RE) power of a signal transmitted through broadcast beams. In the second phase, the RE power of the signal transmitted through the traffic beam is estimated using the Cumulative Distribution Function (CDF) of the antenna boost factor obtained from the broadcast and the traffic envelope radiation patterns made available by the base station vendor. The use of the CDF allows us to mitigate the problems related to the exact estimation of the direction of the measurement point with respect to the beam of the 5G antenna. The method is applied to a real 5G communication system, and the result is compared with the value given by other MPE methods proposed in the literature.

**Keywords:** human exposure assessment; maximum extrapolation procedure; 5G antennas; cellular systems



**Citation:** Schettino, F.; Chirico, G.; D'Elia, C.; Lucido, M.; Pinchera, D.; Migliore, M.D. A Simple and Low-Cost Technique for 5G Conservative Human Exposure Assessment. *Appl. Sci.* **2023**, *13*, 3524. https://doi.org/10.3390/app13063524

Academic Editor: Juan-Carlos Cano

Received: 12 February 2023
Revised: 7 March 2023
Accepted: 8 March 2023
Published: 9 March 2023



## 1. Introduction

5G is a major technological step forward in communication systems [1]. It has introduced a number of new solutions at the physical layer [2–4], sophisticated active large antennas [5–8], and massive MIMO technology [9–11] that take advantage of the presence of scattering objects to obtain multiple spatial channels. The introduction of such technologies has prompted extensive research activity on new large antenna synthesis methods [12–15] and highly precise numerical methods for scattering estimation [16,17] even in anticipation of their use at very high frequencies [18,19]. However, this new technology represents a formidable challenge for the field of human exposure assessment.

Recommended methods for RF exposure are specified in [20]. The document includes three main RF exposure evaluations: product compliance (i.e., determination of the compliance boundary information before the product is placed on the market), product installation compliance (i.e., determinations of the total RF exposure level before the product is put into service) and in situ RF exposure assessment (i.e., after the product has been put into service).

In particular, in [20], the extrapolation of the exposure at the network maximum traffic load and MPE techniques have been introduced. They use a reference signal transmitted at maximum power to estimate the maximum field level assuming that all the resources of the communication system are assigned to a single user. This value is then multiplied by a proper $F_{PR}$ factor according to ([20] clause B5).

Many effective solutions for 5G MPE have been proposed in the literature [21–32], which allow accurate assessment of the field level at the measurement point in currently used 5G systems. They mostly deal with the estimation of the boost factor of traffic beams with respect to broadcast beams (called $F_{beam}$ below; see Section 2). However, the proposed measurement techniques require an active interaction with the gNB and/or expansive measurement setups.

In this paper, we investigate the use of the envelope radiation patterns [33,34] to obtain a conservative value of the field level at the measurement location.

The method is based on a Maximum Power Extrapolation approach. It allows a conservative value of the RF exposure level to be obtained and can be applied to both product compliance and product installation compliance in order to determine if the RF exposure levels are in compliance with exposure limits and regulations.

It requires the measurement of a reference quantity associated with the SS-PBCH (such as PSS, SSS, PBCH, or PBCH-DMRS). This step requires a simple spectrum analyzer and allows the Resource Element (RE) power of a signal transmitted through the Broadcast beam to be obtained. A cheaper approach based on the use of a calibrated cell phone to obtain SS-RSRP can also be followed. In the second phase, the field level is estimated using the CDF of the antenna boost factor obtained from the broadcast and from the traffic envelope radiation patterns made available by the base station vendor [33]. The use of the CDF allows mitigating the problems related to the exact estimation of the direction of the measurement point with respect to the beam of the 5G antenna. The method is applied to a real 5G communication system, and the result is compared with the value given by other MPE methods proposed in the literature.

The value obtained with the procedure described above is an upper bound with a high probability of the maximum field value.

The paper is organized in the following way.

Section 2 introduces the MPE procedure for 5G systems, recalls techniques for antenna boost factor estimation from measurements, and introduces the technique for antenna boost factor estimation from the envelope radiation patterns.

Section 3 describes the MPE procedure based on the antenna boost factor estimated from the envelope radiation patterns.

Section 4 presents an experimental validation of the method.

Section 5 discusses a possible procedure to obtain a conservative and realistic value of the field from the MPE estimation.

Section 6 is devoted to the conclusions.

The description of the frame structure is reported in many books and papers and will not be repeated in this contribution. The reader can find a brief description in the Appendix of Ref. [26].

## 2. Maximum Power Extrapolation Technique for 5G

The goal of the Maximum Power Extrapolation procedure is to estimate the maximum field level (V/m) that can be obtained at the measurement point. This supposes an unrealistic condition in which a single user saturates all the resources of the communication system. As indicated in the introduction, this quantity is used as a reference for estimating the exposure to electromagnetic fields under realistic conditions using an appropriate scale factor.

Loosely speaking, the procedure requires estimating a reference quantity that is a cell-specific signal always "on air" and is transmitted at maximum power. Instruments usually give the power level as it arrives at the instrument's input connector. From this value and

the knowledge of the Antenna Factor [35] and the attenuation of the cable connecting the antenna to the receiver, it is possible to obtain the value of the field level.

Finally, this value is multiplied by proper factors in order to obtain the maximum field level from the measured field level.

In 5G, the maximum EM field level can be estimated as

$$E_{5G}^{max} = E_{SSB} \sqrt{N_{SC}} \sqrt{F_{TDC}} \sqrt{F_{beam}} \quad (1)$$

where $N_{SC}$ is the number of subcarriers in the entire frequency channel, $F_{TDC}$ is the duty cycle when TDD multiplexing is used, and $E_{SSB}$ is the field level of a Resource Elements of the reference signal, which in 5G is an SSB-related quantity. The reference value can also be obtained by the direct measurement of the SSB using scalar analyzers [22]. SSBs are periodically transmitted using broadcast beams also in the absence of user data traffic and consequently are are always "on air".

However, most radio resources are used for user traffic data, which are transmitted using traffic beams (see Figure 1). Since traffic beams have higher gain compared to broadcast beams, the REs of the user traffic data have higher power compared to the ones used in SSBs. $F_{beam}$ is the ratio between the power per RE of the user traffic data and of the SSBs. This quantity is also the ratio between the traffic beam gain and the traffic beam gain in the measurement position.

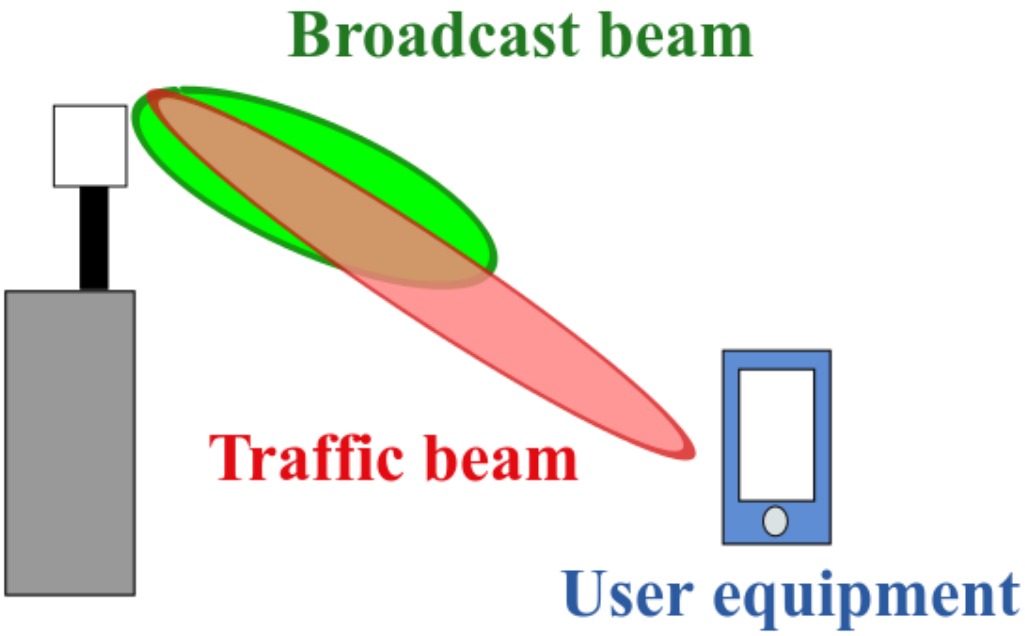


**Figure 1.** 5G uses two different kinds of beamsL the broadcast beams, which have lower directivity and are used to transmit the SSBs, and traffic beams, which have higher directivity and are steered toward the UE to send UE-specific information, such as traffic data [34].

Indeed, the high flexibility of antennas used in 5G represents a huge challenge for $F_{beam}$ estimation. This problem has been successfully addressed in currently deployed 5G systems.

A first possible solution is to perform measurements over a period of time, observing traffic data by waterfall reconstruction [22]. In the case of users requiring connections in the same direction of the measurement points, it is possible to measure the field radiated by traffic beams, and hence the $F_{beam}$ factor.

A different solution, proposed in [24], requires a UE able to force the traffic toward the measurement position. This allows measuring both the broadcast beam level and the

traffic beam level, obtaining the value of $F_{beam}$. A video explaining this method is available in [36].

It should be emphasized that forcing traffic to the measurement point requires actively interacting with the gNB. This also allows access to the rich 5G UE-specific signaling structure (as PDSCH-DMRS, NZ CSI-RS, PDSCH, and CSI-RSRP), opening up further interesting scenarios that require neither a cell reference signal nor $F_{beam}$ estimation [26].

## 3. The Conservative Maximum Power Estimation Procedure

Measurement of $F_{beam}$ is not an easy task. Consequently, solutions that do not require "on-air" measurements to estimate $F_{beam}$ by means of numerical simulations are of great interest.

Unfortunately, information on the configuration of the field radiated by Active Antenna Systems (AASs) [34] provided by the vendors is limited. In particular, the AAS radiation characteristics are summarized by the so-called "Envelope Radiation Pattern" [33], defined as *a non-physical radiation pattern obtained by taking, for each direction in azimuth and elevation, the maximum of the absolute, not peak-normalized to its own peak, radiation pattern among the radiation patterns that the AAS can generate for a given operating condition (deployment/coverage scenario).*

Summarizing the key points reported in [33] that are useful for the problem discussed in this Section, we have the following:

- The Broadcast Envelope Radiation Pattern (BERP) is the envelope pattern of each Broadcast Beam Configuration; since the AAS can have different broadcast configurations available for specific coverage requirements, there are as many BERP as the number of configurations implemented by the AAS.
- The Traffic Envelope Radiation Pattern (TERP) is the envelope pattern of the traffic beams associated with a Broadcast Configuration; TERP could be associated with more than one Broadcast Configuration.
- BERP and TERP are valid in far-field and free-space propagation conditions.
- BERP and TERP can be obtained by measurement or numerical simulation.
- No uncertainty information on BERP and TERP is usually available.
- Information on the mechanical and (if applied) electrical tilting is not included in the data and must be obtained from the operator.

Consequently, the knowledge of the antenna position of the base station and of the measurement position allows us to estimate the parameter $F_{beam}$ from TERP and BERP in the measurement direction in free-space-like conditions, e.g., in the Line of Sight condition with unobstructed first Fresnel ellipsoid, provided that the mechanical and (if applied) electrical inclination of the antenna is known.

In real applications, the field at the observation point is given by the interference of many contributions caused by reflection, refraction, and diffraction phenomena, to which the direct path is added if the propagation is in the LOS (Line of Sight) condition. Multiple reflections cause the presence of fast and slow fading and a significant decrease in the field level in NLOS (Non-Line-of-Sight) conditions compared to propagation in free space. In practice, the enormous flexibility in the choice of beams and the fact that they are provided in free-space conditions make it difficult, if not impossible, to accurately estimate $F_{beam}$ at an observation point from the knowledge of BERP and TERP.

Let $T_{dB}(\theta, \phi)$ and $B_{dB}(\theta, \phi)$ be the TERP and BERP values in the angular direction $\theta, \phi$ of a spherical system centered in the AAS, expressed in dB.

Let

$$T(\theta, \phi) = 10^{T_{dB}(\theta,\phi)/10} \quad (2)$$

$$B(\theta, \phi) = 10^{B_{dB}(\theta,\phi)/10} \quad (3)$$

The scale factor $F_{beam}$ between the Traffic and Broadcast power level can be estimated as the ratio

$$F_{beam}(\theta, \phi) = \frac{T(\theta, \phi)}{B(\theta, \phi)} \tag{4}$$

Envelope radiation patterns can have quite fast variations, especially in the case of broadcast beams (traffic beams are narrow but numerous, so they tend to cover more uniformly the region with respect to Broadcast beams, and their envelope is smoother.). This is a critical problem since a small error in the angular direction of the gNB with respect to the measurement point $(\theta_0, \phi_0)$ can cause a not-negligible error in the estimation of $F_{beam}$. Furthermore, the uncertainty about the angle of inclination of the AAS also causes uncertainty about the exact $(\theta_0, \phi_0)$ value.

To overcome the above problems, in this paper, we will use a statistical approach to estimate an *upperbound* of the boost factor from the antenna data, evaluating the CDF of $F_{beam}(\theta, \phi)$ in an angular region around $(\theta_0, \phi_0)$.

Accordingly, the quantity that will be used in the MPE procedure is the CDF of $F_{beam}(\theta, \phi)$ in an angular region around the measurement point, i.e.,

$$CDF(F_{beam}) = CDF\left(\frac{T(\theta, \phi)}{B(\theta, \phi)}\right) \tag{5}$$

wherein $\theta_i \leq \theta \leq \theta_f$ and $\phi_i \leq \phi \leq \phi_f$, with $\theta_0 \in (\theta_i, \theta_f)$ and $\phi_0 \in (\phi_i, \phi_f)$, are spherical coordinate systems centered in the antenna. Below, we will call $F_{beam}^{0.95}$ the value that is exceeded with a probability less than 0.95.

Furthermore, if only the two main cuts of TERP and BERP are available (as often happens), the CDF will be obtained supposing separable patterns, i.e.,

$$\begin{aligned} T(\theta, \phi) &= T(\theta)T(\phi) \\ B(\theta, \phi) &= B(\theta)B(\phi) \end{aligned} \tag{6}$$

wherein $T(\theta)$ and $B(\theta)$ are the vertical cuts of TERP and BERP, respectively (represented in linear range), and $T(\phi)$ and $B(\phi)$ are the horizontal cuts of TERP and BERP, respectively.

BERP and TERP can be used to obtain a conservative value of the maximum field level that does not require "on air" measurement of $F_{beam}$. Clearly, if the value is within the limit fixed by current regulation, it gives a simple, fast, and low-cost solution to the MPE problem.

The proposed procedure requires, besides the TERP and BERP of the AAS and the angular direction $(\theta_0, \phi_0)$ between the AAS and the measurement point (including tilting angle of the AAS if present), some basic information on the structure of 5G signal:

- Central frequency of the SSB;
- Bandwidth $B$;
- Numerology $\mu$;
- duty cycle $F_{TDC}$.

If not known a priori, these quantities can be obtained by measurements of 5G on-air signals [24].

Furthermore, the procedure requires the measurement of the power-per-resource element of the reference quantity, $P_{RE}^{ref}$. There are many possible solutions to obtain such data. Since the method is conceived as a low-cost solution, the procedure supposes the use of a scalar spectrum analyzer in zero span according to the procedure reported in [22,24].

The steps are as follows:

1. Preliminary calculations of $CDF(F_{beam}(\theta, \phi))$ in different angular ranges.

(a) Load the TERP and BERP data provided by the vendor; transform the values from dB (as usually provided by the vendors) to linear range (see Equation (3)); if only the two principal cuts are available, apply Equation (6); at the end of this step, $T(\theta, \phi)$ and $B(\theta, \phi)$ are available.
(b) Plot the $F_{beam}(\theta, \phi) = T(\theta, \phi)/B(\theta, \phi)$ and identify a suitable number of angular ranges where the function is relatively homogeneous;
(c) For each angular range, evaluate the CDF of the aforementioned quantity; at the end of this step, we have the curves $CDF(F_{beam}(\theta, \phi))$ associated with the different angular ranges.

2. Calculations of useful parameters
   (a) Calculation of the number of subcarriers in the Resolution Bandwidth (RBW) of the Spectrum Analyzer:

$$n_{RBW} = RBW/(15 \times 2^{\mu}) \tag{7}$$

   where $\mu$ is the numerology;
   (b) Calculation of the number of subcarriers of the 5G signal:

$$N_{SC} = B/(15 \times 2^{\mu}) \tag{8}$$

   where $B$ is the bandwidth of the 5G signal;

3. Measurement
   (a) Setting of the Spectrum Analyzer (SA). A description of the scalar spectrum analyzer setting for SSB power measurement is reported in [22,24]. The following setting is suggested: span zero mode, RMS detector, Max Hold mode, and central frequency of the SA equal to the central frequency of the SS-PBCH, RBW equal to 1 MHz.
   (b) Measurement: acquisition of the SSBs power level in zero-span mode and identification of the power level $P^{SSB}$ in dBm of the SSB with the highest power.

4. MPE estimation
   (a) Calculation of the power of a Resource Element associated with the SSB with the highest power as

$$P_{RE}^{SSB} = P^{SSB}/n_{RBW} \tag{9}$$

   (b) Calculation of the field amplitude $E_{RE}^{SSB}$ as

$$E_{RE}^{SSB} = \sqrt{\frac{P_{RE}^{SSB} Z_{in}}{\alpha}} AF \tag{10}$$

   where $Z_{in}$ ($\Omega$) is the input impedance of the instrument, $\alpha$ is the power attenuation of the cable, and $AF$ (1/m) is the Antenna Factor of the antenna connected to the measurement equipment;
   (c) Calculation of the maximum level in the measurement location considering the REs of the broadcast beam

$$E^{max\,SSB} = E_{RE}^{max} \sqrt{N_{SC}} \sqrt{F_{TDC}} \tag{11}$$

   wherein $E_{RE}^{SSB}$ is the power per RE of the signal used as a reference and transmitted along the broadcast beam, and $E^{max\,SSB}$ is the maximum value of the field supposing a fully filled frame where all the REs are transmitted using a broadcast beam.

(d) Identification of the angular range in which the measurement direction $(\theta_0, \phi_0)$ falls and the evaluation of $F_{beam}(\theta_0, \phi_0)$ associated with this angular range is at the desired probability *prob*; let $F_{beam}^{prob}(\theta_0, \phi_0)$ be such a value.

(e) Evaluation of the maximum EMF level in the measurement location with *prob* probability, as

$$E_{5G}^{max\ prob} = E^{max\ SSB} \sqrt{F_{beam}^{prob}(\theta_0, \phi_0)} \tag{12}$$

It is understood that other procedures can be followed to obtain $P_{RE}^{SSB}$. For example, if SS-RSRP is available, steps 2–3 can be substituted by the acquisition of SS-RSRP. Finally, the procedure has been described for one component of the electric field and must be repeated for each of the three components of the electric field [22].

To summarize, the procedure is simple and robust against many problems caused by the flexibility of the 5G standard.

## 4. Experimental Validation of the Procedure

In this section, the procedure is applied step-by-step considering an experimental example. The data reported in Ref. [24] are used, acquired using a Rohde & Schwarz FSP30 spectrum analyzer connected to a Keysight N6850A Broadband Omnidirectional antenna.

The gNB is placed roughly 20 m above ground level, and the angular position of the measurement point with respect to the gNB is ($\phi_0 \simeq 0°$, $\theta_0 \simeq 28°$). The antenna system is an mMIMO 64T64R operating with SU-MIMO.

The basic information on the 5G signal is as follows:

- Central frequency of the SSB: 3649.44 MHz;
- Bandwidth: $B = 80$ MHz;
- Numerology: $\mu = 1$;
- Duty cycle: $F_{TDC} = 0.743$.

More details on the gNB and on the 5G signal can be found in [24].

We consider the MPE with a probability of 95% ($prob = 0.95$).

As a preliminary step, starting from the BERP and TERP of the AAS, the functions $B(\theta, \phi)$ and $T(\theta, \phi)$ (Figure 2) are obtained.

From the plot of $F_{beam}(\theta, \phi)$ (Figure 3), three different angular regions in which the functions show some degree of homogeneity are identified; the regions chosen in this example, indicated as colored rectangles in Figure 2, are as follows (in this example, quite large regions have been chosen; it is understood that it is possible to select narrower regions better centered on the measurement directions.):

- Region A: $0° \leq \theta \leq 12°$, $-40° \leq \phi \leq 40°$
- Region B: $12° \leq \theta \leq 23°$, $-40° \leq \phi \leq 40°$
- Region C: $23° \leq \theta \leq 30°$, $-40° \leq \phi \leq 40°$

In the right part of Figure 3, a contour plot of the $F_{beam}(\theta, \phi)$ restricted to Region C is shown. The function exhibits a quite complex variation. As discussed in the text, the statistical approach allows the problems related to the exact value of the angular position of the UE to be mitigated.

The three CDF curves associated with the three regions are calculated: the curves are shown in Figure 4 (Region A: blue curve, Region B: red curve; Region C: yellow curve).

Regarding the measurements, the settings of the Spectrum Analyzer were as follows: span zero mode, RMS trace, central frequency 3649.44 MHz, and 1 MHz RBW. The plot of the SSBs power (in the absence of active UEs) is shown in Figure 5; the presence of an SSB burst [37] consisting of six SSBs is clearly visible. (After the SSB burst set there are four Tracking Reference Signals [26] signals, which are not of interest in the proposed MPE procedure.); The highest power level of the SSBs is

$$P^{SSB} = -44 \text{ dBm}.$$

Applying the steps listed in the previous Section, we obtain $E^{max\,SSB} = 0.24$ V/m.

The angular direction of the measurement point (i.e., $\theta_0 \simeq 28°, \phi_0 \simeq 0°$) falls in Region C (yellow curve in Figure 4). Choosing 0.95 confidence, we have $F^{0.95}_{beam}(\theta_0, \phi_0) \simeq 120$, i.e., $\sqrt{F^{0.95}_{beam}(\theta_0, \phi_0)} \simeq 11$, and $E^{max\,0.95}_{5G} = 0.24 \times 11 = 2.6$ V/m.

The procedure indicates that the maximum field level in the measurement point is lower than 2.6 V/m in 95% of the positions of Region C.

To validate this result, it is necessary to compare the MPE result (obtained from data acquired in absence-of-data-traffic condition) with the field actually radiated in the case of maximum data traffic load.

In this regard, in the measurement session reported in [24], the communication system was forced to completely fill the frame using a UE terminal. Consequently, it was possible to obtain the maximum field value using Channel Power measurement. The measurement affected by the narrowest uncertainty ([24], Table 3, row 2) indicates a value of the maximum field level in the measurement position equal to $1.72 \pm 0.29$ V/m. The uncertainty range (expanded uncertainty, coverage factor $k = 2$) of this measurement is plotted in Figure 6 as two green lines.

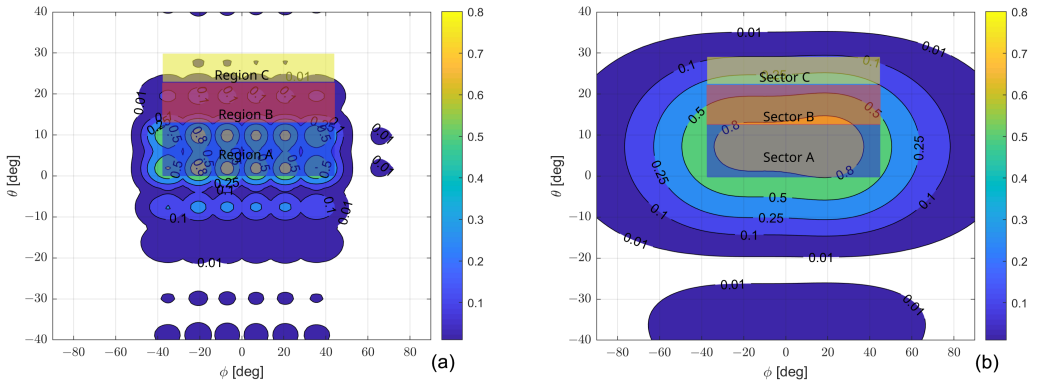


**Figure 2.** $B(\theta, \phi)$ (**a**) and $T(\theta, \phi)$ (**b**) normalized to their maximum represented in color scale according to the colorbar shown on the right; the three regions in which the CDF is estimated are indicated as colored rectangles; the colors of the rectangles are not related to the colorbar on the right.

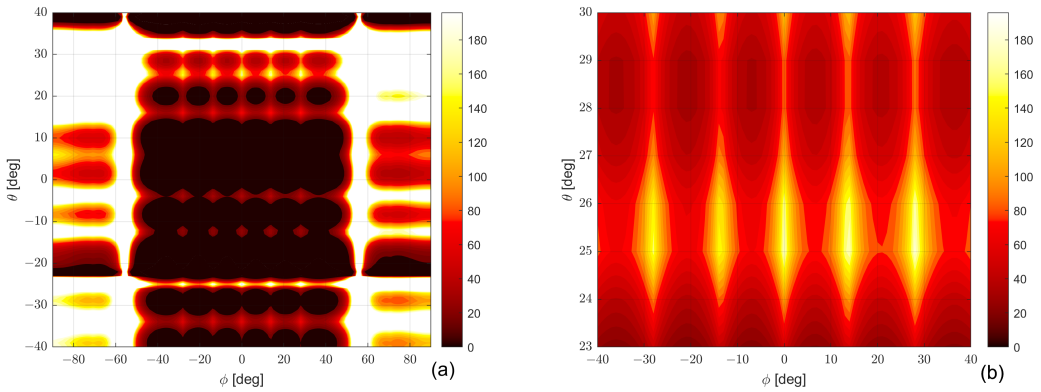


**Figure 3.** (**a**): $F_{beam}(\theta, \phi)$ function; (**b**): $F_{beam}(\theta, \phi)$ function in Region C; the values (in dB) are represented in color scale according to the colorbar shown on the right. The figure shows a fast variation of the function with the angular position of the UE. The statistical approach allows this problem to be mitigated.

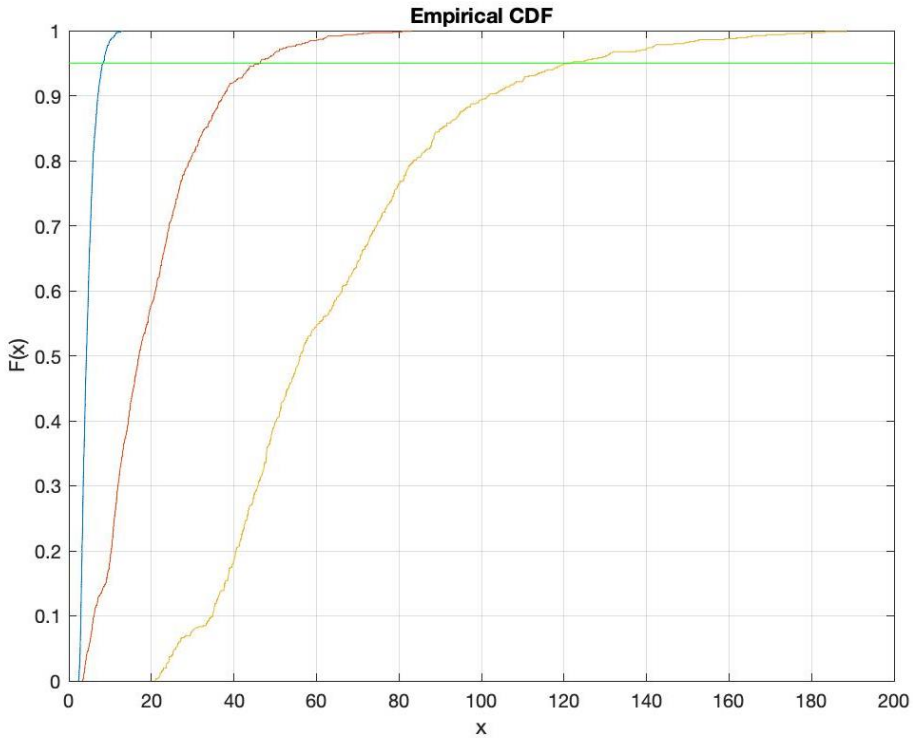


**Figure 4.** CDF of $F_{beam}$; blue: Region A ($0^\circ \leq \theta \leq 12^\circ$, $-40^\circ \leq \phi \leq 40^\circ$); red: Region B ($12^\circ \leq \theta \leq 23^\circ$, $-40^\circ \leq \phi \leq 40^\circ$); yellow: Region C $23^\circ \leq \theta \leq 40^\circ$, $-40^\circ \leq \phi \leq 40^\circ$); the green line indicates the 0.95 probability level.

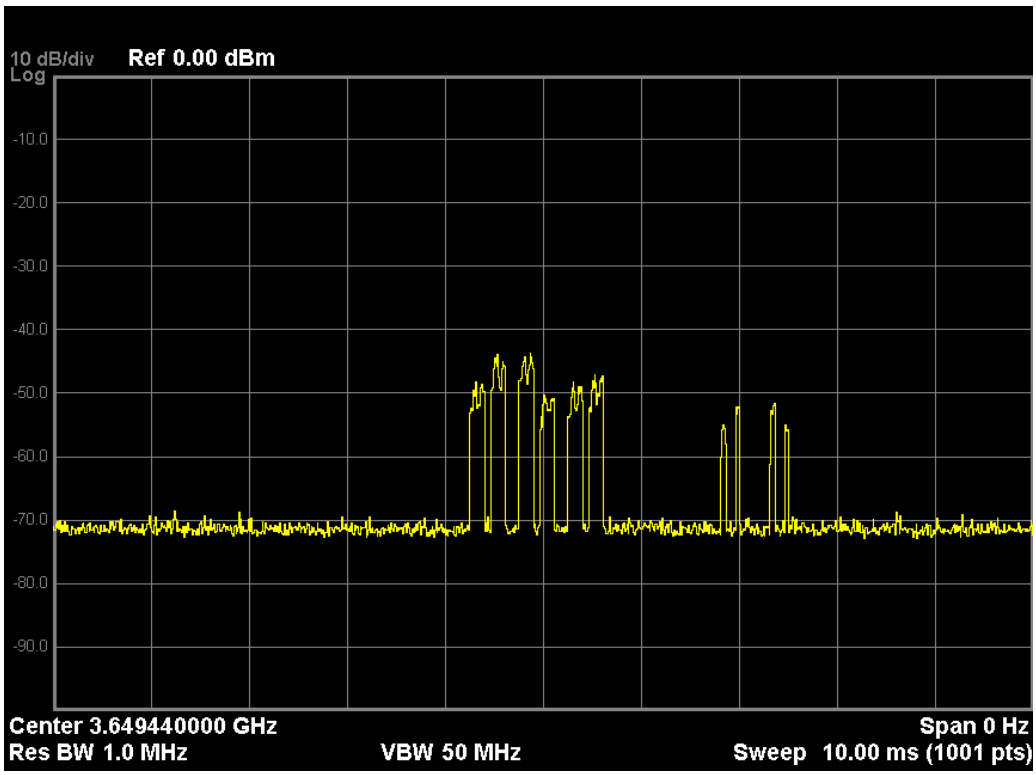


**Figure 5.** Span zero measurement of 5G signal in the absence of active users; the six SSBs are clearly visible, with the highest power observed to be −44 dBm; Tracking Reference Signals are also visible after the SSBs [24,26].

The value obtained from the MPE procedure proposed in this document is plotted as a red square labeled as "Beam Env" in the same figure, i.e., Figure 6. The plot shows that the value is above the uncertainty range, giving a conservative estimation of the field level and confirming the validity of the proposed method.

For comparison, if we apply MPE without the correction of $F_{beam}$ (i.e., only considering SSB-related measurements), we have an underestimation of the maximum field level (dark violet diamond labeled "SSB" in Figure 6), confirming the importance of a correct estimate of the effect of the traffic beams.

It is understood that if the conservative value obtained with the method proposed in this work is higher than the limit set by legislation, more accurate MPE methods must be used to measure the effectiveness of the traffic beam. For completeness, in Figure 6, the results using a number of MPE techniques are shown. These methods are described in detail in [24,26]. In particular, the results shown in Figure 6 have been obtained using the following methods. (The term SSB-related signals denotes the measurement of the PSS or SSS or PBCH or PBCH-DMRS power using a signal analyzer; or the SS-RSRP value obtained using a signal analyzer, a network scanner, or a 5G cellular phone; or the power of the SSB using a spectrum analyzer in zero-span mode.)

1. SSB: MPE from SSB-related signals without $F_{beam}$ correction;
2. Beam Env: the method discussed in this paper, i.e., MPE from SSB-related signals corrected by $F_{beam}$ that is statistically estimated from TERP and BERP using CDF;
3. $F_{beam}$: MPE from SSB-related signals corrected by measured $F_{beam}$ value [24];
4. FR: field level estimated by summing the power of all the REs in the frame using data acquired by signal analyzer [26];
5. CSI-RS: MPE from the power of the REs of the CSI-RS using data acquired with a signal analyzer [26];
6. ZS: MPE from the power of the REs measured using a spectrum analyzer in zero-span mode [26];
7. PDSCH CD: MPE from the power of the REs of the PDSCH directly measured in the Code Domain using the data acquired by a signal analyzer [26];
8. CSI-RSRP: MPE reading the CSI-RSRP acquired using a signal analyzer or network scanner [26];

Finally, as previously pointed out, the two green lines limit the range to which the maximum field value, estimated using Channel Power measurement on fully loaded frames, belongs, with a 95% probability [24].

It is useful to note that the third method ("Fbeam", plotted in pink in the figure) refers to the procedure proposed in [24]. This method includes the measurement of $F_{beam}$. Consequently, we also have an indication of the *actual* $\sqrt{F_{beam}}$ value, which turns out to be $\simeq$6.6. In the present case, the value estimated by means of the proposed method is almost twice the actual value. As a matter of fact, the considered example is the worst case, as we have chosen a measurement point where the variation of $F_{beam}$ is very fast (see Figure 3). Consequently, the uncertainty of the beam direction is more critical, resulting in a rough upper bound. In regions A and B, the estimated value would be much closer to the actual value.

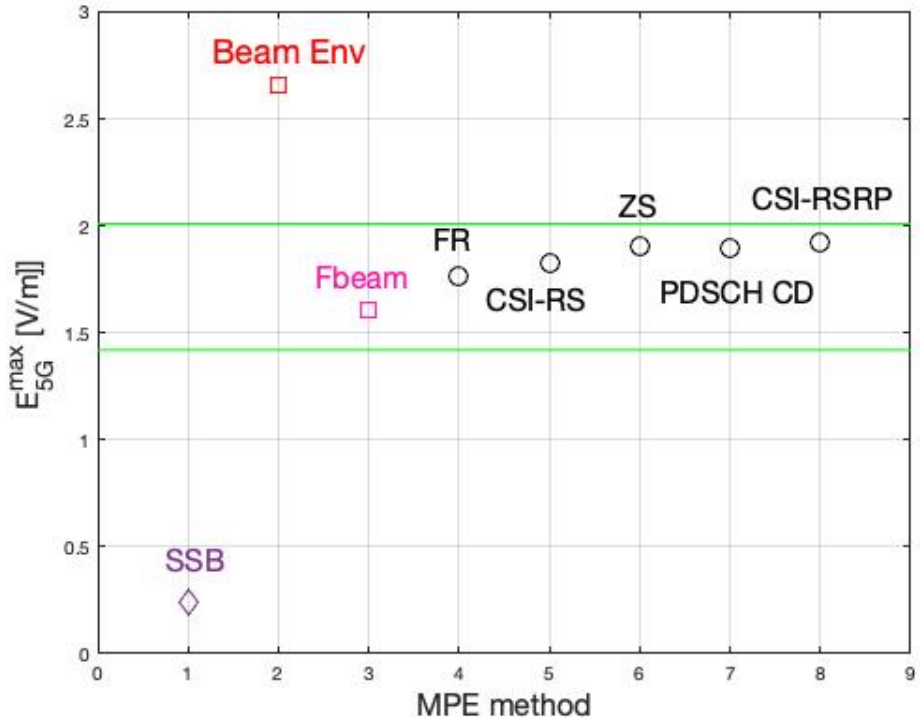


**Figure 6.** Estimated $E_{5G}^{max}$ (V/m) using different methods. SSB/SS-RSRP: EMP from SSB RE power without $F_{beam}$ correction; Beam Env: maximum SSB RE power corrected by $F_{beam}^{0.95}$ obtained from envelope radiation patterns; $F_{beam}$: maximum SSB RE power corrected with measured $F_{beam}$ [24]; FR: value estimated from the REs' power measurement in the whole frame [26]; CSI-RS: values obtained from CSI-RS REs power [26]; ZS: value obtained with Zero Span measurement [26]; PDSCH CD: value obtained from PDSCH RE power measured in the Code Domain [26]; CSI-RSRP: value obtained from CSI-RSRP [26]. The two green lines show the limits range in which the maximum field value belongs with a 95% probability estimated using Channel Power measurement on full-loaded frames [24].

## 5. Estimation of a Realistic Value of the Field Level from the MPE Value

As highlighted in the introduction, the value obtained by the MPE techniques is an unrealistic upper limit, since it assumes that all the resources of the communication system are assigned to a single user for a period of time of 6 or 30 min according to the international guidelines [38]. The MPE value is then scaled according to the national regulations by an appropriate correction factor that takes into account the stochastic nature of the communication process in cellular systems in order to obtain a realistic value. This requires a complex statistical analysis that takes into account the period of time during which the user has access to the communication channel and the radiation characteristics of the traffic beams. An interesting analysis is reported in [39–42].

Following the general simplicity of the approach of this work, we use the formula reported in [43], which provides a simple estimate of the average value of the reduction factor (in power) called $F_{ant}$ in the paper:

$$F_{ant} \simeq \frac{4\pi}{\Omega} \frac{1}{D} \tag{13}$$

where $\Omega$ is the solid angle of the domain served by the antenna and $D$ is the directivity of the beam in the direction of the measurement point. Below, we will suppose that the directivity is almost equal to the gain $G$ of the antenna. This value can be obtained by the plot of the envelope of beams and the knowledge of the maximum gain of the antenna.

The value given by Equation (13) is basically a mean value, while the current regulation requires the correction term to be at 95% probability [20]. However, in [43], it is shown that in the case of a large number of users, Equation (13) gives only a slight underestimation of the value at the 95% probability. In order to take into account this underestimation, we introduce a correction parameter denoted as $F_{corr}$. Accordingly, a conservative value of the level in the measurement point in realistic conditions $E_{5G}^{0.95}$ is obtained by the $E_{5G}^{\max\ 0.95}$ and the Gain of the AAS value is

$$E_{5G}^{0.95} = E_{5G}^{\max\ 0.95} \sqrt{F_{corr}} \sqrt{\frac{4\pi}{\Omega} \frac{1}{D_{eq}}} \tag{14}$$

A comparison with the accurate estimate of the beam-sweep effect using the statistical approach, as obtained in Ref. [41], shows that $s_{ant} = 1.5$ is sufficient to obtain a conservative value of the reduction factor with 0.95 probability [43]. It is understood that if a more accurate estimation of $F_{corr}$ is required, it is possible to consider the specific propagation scenario in the numerical simulation, as shown in [43]. Considering a coverage range of $120^\circ \times 30^\circ$ and the Gain of the antenna, we have

$$E_{5G}^{0.95} = 2.6 \times 0.50 = 1.3\,\mathrm{V/m} \tag{15}$$

For comparison, a (largely) conservative value of the statistical factor is proposed in the technical report IEC62669 [44]. This value provides an estimation of the reduction factor versus the percentage of utilization of the resources of the communication system. In particular, the worst condition is obtained in the case of a large number of users (i.e., almost full use of the resources of the communication system). According to the conservative approach followed in this article, we consider this case. The conservative value of the power reduction factor, in this case, is equal to 0.32, i.e., 0.57 in terms of field reduction, obtaining:

$$E_{5G}^{0.95} = 2.6 \times 0.57 = 1.5\,\mathrm{V/m} \tag{16}$$

## 6. Conclusions

A method to estimate a conservative value of the maximum field level that can be radiated by a 5G base station has been introduced and experimentally validated.

The method is conceived to be simple and low-cost. It requires the broadcast and the traffic Envelop Radiation Patterns and the measurement of a reference value transmitted through the broadcast beams.

In the experimental example, a standard and relatively low-cost scalar spectrum analyzer was used. It is understood that other solutions can be adopted, for example, directly accessing reference signals, but such solutions would require more expensive devices.

With reference to the technology currently used in 5G systems, the main limitation of the proposed procedure is that it gives only a conservative value of the field level. If the limit of the standard is exceeded, it is, therefore, necessary to use other procedures that allow a more precise estimation of the field level.

As noted in the introduction, this paper is closely linked to the two papers [24,26], with which it shares the experimental set-up. The three papers together cover a large number of possible solutions for 5G MPE, giving at the same time a clear idea of the sheer complexity of MPE in 5G. This great complexity is due to the high flexibility of 5G and the limited information on the system status from the UE side, in particular with reference to the AAS configuration during the measurement session.

The enormous difficulties encountered in defining robust MPE 5G extrapolation techniques are a lesson that should be considered in setting the standard for the sixth generation of cellular communications systems.

**Author Contributions:** Conceptualization, M.D.M.; Formal analysis, M.L. and G.C.; Funding acquisition, F.S. and M.L.; Methodology, F.S. and M.D.M.; Supervision, F.S.; Validation, D.P.; Writing—original draft, M.D.M.; Writing—review and editing, C.D. All authors have read and agreed to the published version of the manuscript.

**Funding:** This work is part of the European Union's Horizon Europe research and innovation program under grant agreement No. 101057527 (NextGEM) funded by the European Union. Views and opinions expressed are, however, those of the authors only and do not necessarily reflect those of the European Union. Neither the European Union nor the granting authority can be held responsible for them.

**Informed Consent Statement:** Not applicable.

**Data Availability Statement:** The data presented in this study are available on request from the corresponding author.

**Acknowledgments:** The author thanks Daniele Franci (Arpa Lazio), Settimio Pavoncello (Arpa Lazio), Enrico Grillo (Arpa Lazio), Sara Adda (Arpa Piemonte), Riccardo Suman (Vodafone Italia SpA), Stefano D'Elia (Vodafone Italia SpA), Roberto Cosentino (Rohde Schwarz company), and Massimo Bauco (Rohde Schwarz company) to provide the experimental data and for their invaluable help in analyzing the measured data.

**Conflicts of Interest:** The authors declare no conflict of interest.

## References

1. Zaidi, A.; Athley, F.; Medbo, J.; Gustavsson, U.; Durisi, G.; Chen, X. *5G Physical Layer: Principles, Models and Technology Components*; Academic Press: Cambridge, MA, USA, 2018.
2. Ma, Z.; Zhang, Z.; Ding, Z.; Fan, P.; Li, H. Key techniques for 5G wireless communications: Network architecture, physical layer, and MAC layer perspectives. *Sci. China Inf. Sci.* **2015**, *58*, 041301:1–041301:20. [CrossRef]
3. Medjahdi, Y.; Traverso, S.; Gerzaguet, R.; Shaiek, H.; Zayani, R.; Demmer, D.; Zakaria, R.; Doré, J.B.; Mabrouk, M.B.; Le Ruyet, D.; et al. On the road to 5G: Comparative study of physical layer in MTC context. *IEEE Access* **2017**, *5*, 26556–26581. [CrossRef]
4. Abu-Rgheff, M.A. *5G Physical Layer Technologies*; John Wiley & Sons: Hoboken, NJ, USA, 2019.
5. Hong, W.; Jiang, Z.H.; Yu, C.; Zhou, J.; Chen, P.; Yu, Z.; Zhang, H.; Yang, B.; Pang, X.; Jiang, M.; et al. Multibeam antenna technologies for 5G wireless communications. *IEEE Trans. Antennas Propag.* **2017**, *65*, 6231–6249. [CrossRef]
6. Fager, C.; Eriksson, T.; Barradas, F.; Hausmair, K.; Cunha, T.; Pedro, J.C. Linearity and efficiency in 5G transmitters: New techniques for analyzing efficiency, linearity, and linearization in a 5G active antenna transmitter context. *IEEE Microw. Mag.* **2019**, *20*, 35–49. [CrossRef]
7. Pinchera, D.; Migliore, M.D.; Schettino, F. Optimizing antenna arrays for spatial multiplexing: Towards 6G systems. *IEEE Access* **2021**, *9*, 53276–53291. [CrossRef]
8. Maldonado, G.; Maldonado, A.R.; Balderas, L.I.; Panduro, M.A. Time-Modulated Antenna Arrays for Ultra-Wideband 5G Applications. *Micromachines* **2022**, *13*, 2233. [CrossRef]
9. Mumtaz, S.; Rodriguez, J.; Dai, L. *MmWave Massive MIMO: A Paradigm for 5G*; Academic Press: Cambridge, MA, USA, 2016.
10. Prasad, K.S.V.; Hossain, E.; Bhargava, V.K. Energy efficiency in massive MIMO-based 5G networks: Opportunities and challenges. *IEEE Wirel. Commun.* **2017**, *24*, 86–94. [CrossRef]
11. Chataut, R.; Akl, R. Massive MIMO systems for 5G and beyond networks—Overview, recent trends, challenges, and future research direction. *Sensors* **2020**, *20*, 2753. [CrossRef]
12. Aslan, Y.; Puskely, J.; Janssen, J.; Geurts, M.; Roederer, A.; Yarovoy, A. Thermal-aware synthesis of 5G base station antenna arrays: An overview and a sparsity-based approach. *IEEE Access* **2018**, *6*, 58868–58882. [CrossRef]
13. Anselmi, N.; Gottardi, G.; Rocca, P.; Oliveri, G.; Massa, A. Unconventional M-MIMO phased array design for 5G wireless systems. In Proceedings of the 2019 IEEE International Symposium on Phased Array System & Technology (PAST), Waltham, MA, USA, 15–18 October 2019; pp. 1–3.
14. Buttazzoni, G.; Babich, F.; Vatta, F.; Comisso, M. Geometrical synthesis of sparse antenna arrays using compressive sensing for 5G IoT applications. *Sensors* **2020**, *20*, 350. [CrossRef]
15. Pinchera, D.; Migliore, M.D.; Panariello, G. Isophoric inflating deflating exploration algorithm (i-idea) for equal-amplitude aperiodic arrays. *IEEE Trans. Antennas Propag.* **2022**, *70*, 10405–10416. [CrossRef]
16. Lucido, M.; Schettino, F.; Migliore, M.D.; Pinchera, D.; Di Murro, F.; Panariello, G. Electromagnetic scattering by a zero-thickness PEC annular ring: A new highly efficient MoM solution. *J. Electromagn. Waves Appl.* **2017**, *31*, 405–416. [CrossRef]
17. Lucido, M.; Schettino, F.; Panariello, G. Scattering from a thin resistive disk: A guaranteed fast convergence technique. *IEEE Trans. Antennas Propag.* **2021**, *69*, 387–396. [CrossRef]
18. Dukhopelnykov, S.V.; Sauleau, R.; Nosich, A.I. Integral equation analysis of terahertz backscattering from circular dielectric rod With partial graphene cover. *IEEE J. Quantum Electron.* **2020**, *56*, 1–8. [CrossRef]

19. Dukhopelnykov, S.V.; Lucido, M.; Sauleau, R.; Nosich, A.I. Circular dielectric rod with conformal strip of graphene as tunable terahertz antenna: Interplay of inverse electromagnetic jet, whispering gallery and plasmon effects. *IEEE J. Sel. Top. Quantum Electron.* **2021**, *27*, 1–8. [CrossRef]
20. *IEC 62232:2022*; Determination of RF Field Strength, Power Density and SAR in the Vicinity of Radiocommunication Base Stations for the Purpose of Evaluating Human Exposure. IEC: Geneva, Switzerland, 2022.
21. Pawlak, R.; Krawiec, P.; Żurek, J. On measuring electromagnetic fields in 5G technology. *IEEE Access* **2019**, *7*, 29826–29835. [CrossRef]
22. Aerts, S.; Verloock, L.; Van Den Bossche, M.; Colombi, D.; Martens, L.; Törnevik, C.; Joseph, W. In-situ measurement methodology for the assessment of 5G NR Massive MIMO base station exposure at sub-6 GHz frequencies. *IEEE Access* **2019**, *7*, 184658–184667. [CrossRef]
23. Keller, H. On the assessment of human exposure to electromagnetic fields transmitted by 5G NR base stations. *Health Phys.* **2019**, *117*, 541–545. [CrossRef]
24. Adda, S.; Aureli, T.; D'Elia, S.; Franci, D.; Grillo, E.; Migliore, M.D.; Pavoncello, S.; Schettino, F.; Suman, R. A Theoretical and Experimental Investigation on the Measurement of the Electromagnetic Field Level Radiated by 5G Base Stations. *IEEE Access* **2020**, *8*, 101448–101463. [CrossRef]
25. Aerts, S.; Deprez, K.; Colombi, D.; Van den Bossche, M.; Verloock, L.; Martens, L.; Törnevik, C.; Joseph, W. In Situ Assessment of 5G NR Massive MIMO Base Station Exposure in a Commercial Network in Bern, Switzerland. *Appl. Sci.* **2021**, *11*, 3592. [CrossRef]
26. Migliore, M.D.; Franci, D.; Pavoncello, S.; Grillo, E.; Aureli, T.; Adda, S.; Suman, R.; D'Elia, S.; Schettino, F. A New Paradigm in 5G Maximum Power Extrapolation for Human Exposure Assessment: Forcing gNB Traffic Toward the Measurement Equipment. *IEEE Access* **2021**, *9*, 101946–101958. [CrossRef]
27. Kopacz, T.; Schießl, S.; Schiffarth, A.M.; Heberling, D. Effective SSB Beam Radiation Pattern for RF-EMF Maximum Exposure Assessment to 5G Base Stations Using Massive MIMO Antennas. In Proceedings of the 2021 15th European Conference on Antennas and Propagation (EuCAP), Dusseldorf, Germany, 22–26 March 2021; pp. 1–5.
28. Lee, A.K.; Jeon, S.B.; Choi, H.D. EMF Levels in 5G New Radio Environment in Seoul, Korea. *IEEE Access* **2021**, *9*, 19716–19722. [CrossRef]
29. Jiang, T.; Skrivervik, A.K. Assessment of the Electromagnetic Field Exposure due to 5G Base Stations using a Monte-Carlo Method: Initial Results. In Proceedings of the 2021 15th European Conference on Antennas and Propagation (EuCAP), Dusseldorf, Germany, 22–26 March 2021; pp. 1–4.
30. Bornkessel, C.; Kopacz, T.; Schiffarth, A.M.; Heberling, D.; Hein, M.A. Determination of Instantaneous and Maximal Human Exposure to 5G Massive-MIMO Base Stations. In Proceedings of the 2021 15th European Conference on Antennas and Propagation (EuCAP), Dusseldorf, Germany, 22–26 March 2021; pp. 1–5.
31. Adda, S.; Aureli, T.; Bastonero, S.; D'Elia, S.; Franci, D.; Grillo, E.; Migliore, M.D.; Pasquino, N.; Pavoncello, S.; Schettino, F.; et al. Methodology Based on Vector and Scalar Measurement of Traffic Channel Power Levels to Assess Maximum Exposure to Electromagnetic Radiation Generated by 5G NR Systems. *IEEE Access* **2022**, *10*, 12125–12136. [CrossRef]
32. Migliore, M.D.; Franci, D.; Pavoncello, S.; Aureli, T.; Merli, E.; Lodovisi, C.; Chiaraviglio, L.; Schettino, F. Application of the Maximum Power Extrapolation Procedure for Human Exposure Assessment to 5G Millimeter Waves: Challenges and Possible Solutions. *IEEE Access* **2022**, *10*, 103438–103446. [CrossRef]
33. Alliance, N. Recommendation on Base Station Active Antenna System Standards. 2021. Available online: https://www.ngmn.org/publications/basta-active-antenna-systems-v1-0.html (accessed on 10 February 2023).
34. Asplund, H.; Astely, D.; von Butovitsch, P.; Chapman, T.; Frenne, M.; Ghasemzadeh, F.; Hagström, M.; Hogan, B.; Jöngren, G.; Karlsson, J.; et al. *Advanced Antenna Systems for 5G Network Deployments: Bridging the Gap between Theory and Practice*; Academic Press: Cambridge, MA, USA, 2020.
35. Paul, C.R. *Introduction to Electromagnetic Compatibility*; John Wiley & Sons: Hoboken, NJ, USA, 2006; Volume 184.
36. WEB Site. Available online: https://sites.google.com/unicas.it/electromagnetic-information/home (accessed on 1 March 2021).
37. 3GPP. Radio Transmission and Reception (Release 15), 3GPP Technical Specification Group Radio Access Network. NR, TS 38.104, V15.5.0, May 2019. Available online: https://www.etsi.org/deliver/etsi_ts/138100_138199/138104/15.05.00_60/ts_138104v150500p.pdf (accessed on 1 March 2023).
38. International Commission on Non-Ionizing Radiation Protection. Guidelines for limiting exposure to Electromagnetic Fields (100 kHz to 300 GHz). *Health Phys.* **2020**, *118*, 483–524. [CrossRef] [PubMed]
39. Baracca, P.; Weber, A.; Wild, T.; Grangeat, C. A statistical approach for RF exposure compliance boundary assessment in massive MIMO systems. In Proceedings of the WSA 2018; 22nd International ITG Workshop on Smart Antennas, Bochum, Germany, 14-16 March 2018; pp. 1–6.
40. Colombi, D.; Joshi, P.; Xu, B.; Ghasemifard, F.; Narasaraju, V.; Törnevik, C. Analysis of the Actual Power and EMF Exposure from Base Stations in a Commercial 5G Network. *Appl. Sci.* **2020**, *10*, 5280. [CrossRef]
41. Pinchera, D.; Migliore, M.D.; Schettino, F. Compliance Boundaries in 5G Communication Systems: A Statistical Approach. *IEEE Access* **2020**, *1*, 620–628.
42. Schiavoni, A.; Bastonero, S.; Lanzo, R.; Scotti, R. Methodology for electromagnetic field exposure assessment of 5G massive MIMO antennas accounting for spatial variability of radiated power. *IEEE Access* **2022**, *10*, 70572–70580. [CrossRef]

43. Migliore, M.D.; Schettino, F. Power Reduction Estimation of 5G Active Antenna Systems for Human Exposure Assessment in Realistic Scenarios. *IEEE Access* **2020**, *8*, 220095–220107. [CrossRef]
44. *IEC 62669:2019*; Case Studies Supporting IEC 62232—Determination of RF Field Strength, Power Density and SAR in the Vicinity of Radiocommunication Base Stations for the Purpose of Evaluating Human Exposure. IEC: Geneva, Switzerland, 2019.